PROCEEDINGS, Thirty-Second Workshop on Geothermal Reservoir Engineering
Stanford University, Stanford, California, January 22-24, 2007
SGP-TR-183

TRIPLE POROSITY MODEL-DUAL PERMEABILITY WITH TRANSIENT HYDRAULIC DIFFUSIVITY IN NATURALLY FRACTURED RESERVOIRS

Héctor Pulido[1], Fernando Samaniego V.[2], Héber Cinco-Ley[1,2], Jesús Rivera[2], and Guadalupe Galicia[2]

1. Pemex, 2. UNAM
e-mail: hcpulidob@pep.pemex.com

ABSTRACT

Constant flow rate solutions are presented for a triple porosity model-dual permeability using the transient interporosity flow and a skin between two media in mention for to generate a pseudosteady interporosity flow. Transient interporosity flow is modeled in a convolution form, considering matrix, microfractures, vugs and fractures flow. New solutions are presented for two cases, where there is no primary flow through the microfractures and where the compressive and distensive strength process has created an interconnected system of microfractures. In both cases there is an interaction between matrix, microfractures, and fracture systems.
Due to the total diffusivity hydraulic depends on fracture pressure is modeled in a convolution form in combination with a partial derivative of fracture pressure with respect to dimensionless time for to incorporate the ***geometry changes in fractures*** during the production and depletion.

The numerical inversion was carried out with Stehfest's algorithm. In addition, approximate analytical solution for short and long dimensionless time are obtained and compared with the solution calculated by numerical inversion, providing satisfactory results. The values of the numerical inversion were used to generate the results, presented in terms of the dimensionless groups derived from the approximate analytical solution.

Introduction

In areas without cores, open-hole wireline logs may be used to help identify vugs zones; however, vugs are not always recognized by conventional logs because of their limited vertical resolution. Vugs porosity is common in many reservoirs and its importance in the petrophysical and productive characteristics of a rock has been recognized in several works. Vugs porosity can be subdivided into small and large types. Vugs effect on permeability is related to their connectivity[3]. One purpose of our work is to present a technique to identify high secondary porosity, mainly vugs porosity.

When dealing with NFR, it is important to study its origin and main characteristics, such as the regularity of their distribution, and morphology, aperture, width, etc. Figs. 1 and 2 presents photographs of whole cores taken in highly productive naturally fractured carbonate vuggy and fractured formations. Fig. 1.a shows two fracture system, one being vertical and the other inclined, connected through vugs. Fig. 1.b illustrates a fracture system that has a main vertical direction. Fig. 1.c shows a system of vertical and conjugate fractures; some vugs can be observed and an open fracture of aperture of about 3mm.

Fig. 2 shows three additional images of carbonate whole cores. Fig. 2.a illustrates the case of fractures filled by calcite. Fig 2.b presents the important physical condition of fracture planes affected by dissolution, which increases both secondary porosity and bulk permeability. Finally, Fig. 2.c exhibits vertical fractures, enhanced by dissolution vugs, which improve the formation bulk conductivity.

It has been observed in the literature that vugs zones strongly influence production performance[3, 4].

Recently two papers have discussed results strictly related to the presents study. Camacho etal[1]. developed a new way to model the secondary porosity of naturally reservoirs (NFR), mainly vuggy porosity the authors derived solutions for two cases, one where there is no primary flow through the vugs (which is an improvement of the Warren and Root model), and second in which the dissolution process of the pore volume has resulted in an interconnected system of vugs and caves. Thus, this is a triple-porosity / dual permeability model.

Rodriguez et al [2]. developed a nested – triple – porosity single – permeability model for the pressure transient behavior of a well producing in a NFR, there porosity systems, acting at different scales, are assumed to coexist in these reservoirs: matrix, small scale and large scale secondary porosity media, flow in series among these media is considered; the matrix exchanges fluids whit the small - scale secondary porosity, which in turn feeds the large – scale secondary porosity. The first two media are assumed to have a local effect on fluid flow, and are considered as discontinuous, while the third, the large – scale secondary porosity medium, is considered to

affect fluid flow at the reservoir scale and it is consequently continuous.

The present paper addresses the problem of modeling vugs in naturally fractured reservoirs, allowing the possibility of primary flow through vugs, and develops a method to identify vugs in reservoirs through well test and decline curves analysis evaluating porosity associated with vugs and fractures, and determining vugs connectivity.

Results

This section is divided in two parts. The first part presents the formulation of the model. The second part presents the pressure behavior during the transient period, for both dual and single-permeability models.

Model Formulation

In this work, a triple porosity model-dual permeability is proposed using the transient interporosity flow approximation and a skin between the two media in mention for to generate a pseudosteady interporosity flow. In this model is necessary the geometry and form of the matrix and vugs. The pseudosteady fluid transfer between matrix, vugs, and fractures systems is directly proportional to the difference in the volume average macroscopic matrix, vugs, and fractures pressure. A free interaction between matrix, vugs, and fractures systems is allowed when the skin is zero between two media ***and changes in properties with time of fractures hydraulic diffusivity***. This is different from the model proposed in Abdassah and Esshaghi[6], and for this reason the triple porosity model proposed in this work is unique.

Radial flow in the *large* scale secondary porosity media with two source term in convolution form is described in dimensionless variables, ***and changes in properties with time of fractures hydraulic diffusivity*** is modeled in a convolution form for the triple porosity-dual permeability model, is given as follows:

Considering a cylindrical symmetry, *the differential equation for the fractures (large scale)*, using dimensionless variables, for the triple porosity–dual permeability model, is given as follows:

$$\kappa\left[\frac{\partial^2 p_{FD}(r_D,t_D)}{\partial r_D^2}+\frac{1}{r_D}\frac{\partial p_{FD}(r_D,t_D)}{\partial r_D}\right]$$
$$-\omega_f(t_D)C_{fFbD}\frac{\partial p_{FD}(r_D,t_D)}{\partial t_D}*\frac{F_{fF}(\eta_{fD},t_D)}{1+S_{fF}F_{fF}(\eta_{fD},t}$$
$$-\omega_m(t_D)C_{mFbD}\frac{\partial p_{FD}(r_D,t_D)}{\partial t_D}*\frac{F_{mF}(\eta_{mD},t_D}{1+S_{mF}F_{mF}(\eta_{mD}}$$
$$=\int^{t_D}\omega_F(t_D-\tau)\frac{\partial p_{FD}(r_D,\tau)}{\partial \tau}d\tau \quad (1)$$

Where $F_{mF}(\eta_{mD})$ and $F_{fF}(\eta_{mD})$ are the source functions for matrix and vugs.

Source functions for matrix and vugs.

Transient matrix-fracture linear flow:

$$F_{mF}(\eta_{mFD},t_D)=4\eta_{mFD}\sum_{n=1}^{\infty}e^{-\eta_{mFD}(2n+1)^2\pi^2(t_D-\tau)} \quad (2)$$

Transient vugs-fractures spherical flow:

$$F_{fF}(\eta_{fFD},t_D)=4\eta_{fFD}\sum_{n=0}^{\infty}e^{-\eta_{fFD}(n)^2\pi^2(t_D-\tau)} \quad (3)$$

Initial condition:

$$p_{FD}(r_D,0)=0 \quad (4)$$

Internal boundary condition: constant flow rate:

$$\frac{\partial p_{FD}(1,t_D)}{\partial r_D}=-1 \quad (5)$$

External boundary condition: Infinite reservoir

$$\lim_{r_D\to\infty}p_{FD}(r_D,t_D)=0 \quad (6)$$

Radial flow in the small scale secondary porosity (vugs) is given by:

$$[1-\kappa]\left[\frac{\partial p^2{}_{fD}(r_D,t_D)}{\partial r_D^2}+\frac{1}{r_D}\frac{\partial p_{fD}(r_D,t_D)}{\partial r_D}\right]$$
$$-\omega_F(t_D)C_{fFbD}\frac{\partial p_{fD}(r_D,t_D)}{\partial \tau}*\frac{F_{fF}(\eta_{fD},t_D)}{1+S_{fF}F_{fF}(\eta_{fD},t_D)}$$
$$-\omega_m(t_D)C_{mfbD}\frac{\partial p_{fD}(r_D,t_D)}{\partial \tau}*\frac{F_{mf}(\eta_{mD},t_D)}{1+S_{mf}F_{mf}(\eta_{mD},t_D)}$$
$$=\omega_f(t_D)*\frac{\partial p_{fD}(r_D,t_D)}{\partial t_D} \quad (7)$$

The transient linear flow matrix-vugs transfer:

$$F_{mf}\left(\eta_{mfD},t_D\right)=4\eta_{mfD}\sum_{n=1}^{\infty}e^{-\eta_{mfD}(2n+1)^2\pi^2(t_D)}dt_D$$

Initial condition:

$$p_{fD}(r_D,0)=0$$

Internal boundary condition: constant flow rate:

$$\frac{\partial p_{fD}(1,t_D)}{\partial r_D}=-1$$

External boundary condition: Infinite reservoir

$$\lim_{r_D\to\infty} p_{fD}\left(r_D,t_D\right)=0$$

The porosities are defined by:
Small scale porosity (vugs):

$$\phi_{fb}=\frac{V_{pf}}{V_b}$$

Large scale secondary porosity (fractures):

$$\phi_{Fb}=\frac{V_{pF}}{V_b}$$

Matrix porosity when uses the reference bulk rock:

$$\phi_{mb}=\frac{V_{pm}}{V_b}$$

Total porosity:

$$\phi_t=\phi_{mb}+\phi_{Fb}+\phi_{fb}$$

Matrix area exposed to large scale secondary porosity (fractures):

$$c_{mFb}=\frac{A_{mF}}{V_b}$$

Matrix area exposed to small scale secondary porosity (vugs):

$$c_{mfb}=\frac{A_{mf}}{V_b}$$

Vugs area exposed to large scale secondary porosity (fractures):

$$c_{fFb}=\frac{A_{fF}}{V_b}$$

Interporosity flow shape factor between medium i and medium j.

(8) $$\sigma_{ij}=\frac{A_{ij}}{V_b l_{cij}}=\frac{C_{ijb}}{l_{cij}};$$ (22)

Example, for for cubic matrix and vugs:

(9) $$\sigma_{ij}=\frac{6H^2}{H^3(H/2)}=\frac{12}{H^2}$$

(10) $$\sigma_{ij}=\frac{4\pi r^2}{[4/3\pi r_v^3]}=\frac{3}{r_v^2}=\frac{12}{d_v^2}$$ (23)

Where the dimensionless variables are given by

(11) $$r_D=\frac{r}{r_w}$$ (24)

$$t_D=\frac{[k_{Fb}+k_{fb}]t}{[\phi_{Fb}c_{tFb}+\phi_{mb}c_{tmb}+\phi_{fb}c_{tfb}]\mu r_w^2}$$ (25)

(12) $$p_{FD}=\frac{2\pi[k_{Fb}+k_{fb}]h[p_i-p_F(r,t)]}{q\mu}$$ (26)

$$p_{mD}=\frac{2\pi[k_{Fb}+k_{fb}]h[p_i-p_m(r,t)]}{q\mu}$$ (27)

(13) $$p_{fD}=\frac{2\pi[k_{Fb}+k_{fb}]h[p_i-p_f(r,t)]}{q\mu}$$ (28)

The storativity ratios, for matrix, fractures and vugs are functions of time:

(14) $$\omega_F(t_D)=\frac{\phi_{Fb}c_{tFb}}{\phi_{Fb}c_{tFb}+\phi_{mb}c_{tmb}+\phi_{fb}c_{tfb}}=\omega_{Fi}(t_D)^{-a}$$ (29)

(15) $$\omega_m(t_D)=\frac{\phi_{mb}c_{tmb}}{\phi_{Fb}c_{tFb}+\phi_{mb}c_{tmb}+\phi_{fb}c_{tfb}}=\omega_{mi}(t_D)^{-b}$$ (29)

(19) $$\omega_f(t_D)=\frac{\phi_{fb}c_{tfb}}{\phi_{Fb}c_{tFb}+\phi_{mb}c_{tmb}+\phi_{fb}c_{tfb}}=\omega_{fi}(t_D)^{-c}$$ (30)

(20) Using the porosities can be demonstrated that:

$$\omega_m(t_D)+\omega_f(t_D)+\omega_F(t_D)=1$$ (18)

With $k_{fF}=k_f$ if $p_f>p_F$, and $k_{fF}=k_F$ otherwise.

(21) Note that in the definitions of λ_{mF} and λ_{mf}, we have used k_m because in the absence of capillary forces we expect that under production conditions fluid goes from matrix to vugs and fracture networks.

For the case of the triple porosity-single permeability model, i.e. when there is only primary

flow through the fractures or through the vugs network, the vugs and fractures permeability, respectively, in the above definitions is set equal to zero except in the numerator of λ_{fF}. For these cases $\kappa = 1$ and 0, respectively.
Thus, the parameter κ takes values between zero and one.

$$\kappa = \frac{k_{Fb}}{k_{Fb} + k_{fb} + k_m}$$

Dimensionless matrix area exposed to large scale secondary porosity:

$$C_{mFbD} = \frac{C_{mFb}\, l_c V_b}{V_m} = \frac{A_{mF}\, l_{cmF}}{V_m}$$

Dimensionless matrix area exposed to small scale secondary porosity:

$$C_{mfbD} = \frac{C_{mfb}\, l_c V_b}{V_m} = \frac{A_{mf}\, l_{cmf}}{V_m}$$

Dimensionless vugs area exposed to large scale secondary porosity:

$$C_{fFbD} = \frac{C_{fFb}\, l_c V_b}{V_m} = \frac{A_{fF}\, l_{cfF}}{V_m}$$

Dimensionless diffusivity:

$$\eta_{fFbD} = \frac{\eta_{fb}\, r_w^2}{\eta_{Fb}\, l_{cfF}^{\,2}} = \frac{k_{fb}(\phi c_t)_{Fb}\, r_w^2}{k_{Fb}(\phi c_t)_{fb}\, l_{cfF}^{\,2}}$$

$$\eta_{mFbD} = \frac{\eta_{mb}\, r_w^2}{\eta_{Fb}\, l_{cmF}^{\,2}} = \frac{k_{mb}(\phi c_t)_{Fb}\, r_w^2}{k_{Fb}(\phi c_t)_{mb}\, l_{cmF}^{\,2}}$$

$$\eta_{mfbD} = \frac{\eta_{mb}\, r_w^2}{\eta_{fb}\, l_{cmf}^{\,2}} = \frac{k_{mb}(\phi c_t)_{fb}\, r_w^2}{k_{fb}(\phi c_t)_{mb}\, l_{cmf}^{\,2}}$$

The complete solution in real time is:

$$p_{wD}(t_D) = \frac{1}{2}\left[\ln(t_D) + 0.80907\right] + \frac{1}{2}\left[-E_i\left(\frac{-C_{fFbD}(t_D)\eta_{fFbD}(t_D)t_D}{S_{fF}\left[1-\omega_f(t_D)-\omega_F(t_D)\right]}\right) + E_i\left(\frac{-C_{fFbD}(t_D)\eta_{fFbD}(t_D)t_D}{S_{fF}\omega_f(t_D)\left[1-\omega_f(t_D)-\omega_F(t_D)\right]}\right)\right] + \frac{1}{2}\left[-E_i\left(\frac{-C_{mFbD}(t_D)\eta_{mFbD}(t_D)t_D}{S_{mF}\left[1-\omega_f(t_D)-\omega_F(t_D)\right]}\right) + E_i\left(\frac{-C_{mFbD}(t_D)\eta_{mFbD}(t_D)t_D}{S_{mF}\omega_F(t_D)\left[1-\omega_f(t_D)-\omega_F(t_D)\right]}\right)\right] \quad (41)$$

Petrophysical characterization show that several functions are pseudolinear:

$$p_{wD}(t_D) = \frac{1}{2}\left[\ln(t_D) + 0.80907\right] + \frac{1}{2}\left[-E_i\left(\frac{-C_{fFbDi}\eta_{fFbDi}t_D}{S_{fF}\left[1-\omega_{fi}-\omega_{Fi}\right]}\right) + E_i\left(\frac{-C_{fFbDi}\eta_{fFbDi}t_D}{S_{fF}\omega_{fi}\left[1-\omega_{fi}-\omega_{Fi}\right]}\right)\right] + \frac{1}{2}\left[-E_i\left(\frac{-C_{mFbDi}\eta_{mFbDi}t_D}{S_{mF}\left[1-\omega_{fi}-\omega_{Fi}\right]}\right) + E_i\left(\frac{-C_{mFbDi}\eta_{mFbDi}t_D}{S_{mF}\omega_{Fi}\left[1-\omega_{fi}-\omega_{Fi}\right]}\right)\right] \quad (41)$$

Appendix A presents details of the solution in Laplace space for the triple porosity-single permeability model, considering constant flow rate and an infinite reservoir.

If all secondary porosity (vugs, microfractures and fractures) are lumped, Eq. 41 can written as:

$$p_{wD}(t_D) = \frac{1}{2}\left[\ln(t_D) + 0.80907\right] + \frac{1}{2}\left[-E_i\left(\frac{-C_{mFbDi}\eta_{mFbDi}t_D}{S_{mF}\left[1-\omega_{Fi}\right]}\right) + E_i\left(\frac{-C_{mFbDi}\eta_{mFbDi}t_D}{S_{mF}\omega_{Fi}\left[1-\omega_{Fi}\right]}\right)\right] \quad (42)$$

Using in Eq. 42 the definition of the interporosity flow coefficient λ *as definited by Cinco and Samaniego:*

$$\lambda_i = \frac{C_{mFbDi}\eta_{mFbDi}}{S_{mF}}, \quad (43)$$

the well known Warren and Root Solution is obtained:

$$p_{wD}(t_D) = \frac{1}{2}\left[\ln(t_D) + 0.80907\right] + \frac{1}{2}\left[-Ei\left(\frac{-\lambda_i t_D}{1-\omega_i}\right) + Ei\left(\frac{-\lambda_i t_D}{\omega_i\left[1-\omega_i\right]}\right)\right] \quad (44)$$

Transient Well Test Behavior

It is shown that this solution, given by Eqs. (A-16) or (A-17), extends the typical Warren and Root (1963) solution[5]. Figures 3-5 present analytical results obtained by applying Stehfest algorithm to Eq. (A-16) for different values of the parameters: λ_{mF}, λ_{fF} y λ_{mf}, ω_F, and ω_f, considering that wellbore storage and skin are zero. In all cases the solution of Cinco and Samaniego with $S_{mf} \approx 10$ is represented by the continuous line without symbols. At early times a semilog straight line can be observed. The

presence of an early semilogarthmic straight line indicates the fractures-controlled flow period.

At late times, a straight line parallel to the early-time line represents the homogenous flow period of the fractures, vugs, and matrix blocks, where pressure in fractures, vugs, and matrix, is the same (see Fig. 4).

In a most curves presented in Figs. 3-5, there are anomalous slope changes during the transition period caused by the presence of vugs. In some cases, another intermediate straight line, parallel to the above straight line, is present during this transition period.

This behavior is different in the double-porosity response. Before and after this intermediate straight line there are transition periods, whose slopes may be different from the characteristic constant pressure drop period of Warren and Root shown by the solution. During these transition periods, apparent straight lines may be fitted, with slope ratios that could be 2:1 for the early, intermediate, or late-time segments, which could be interpreted as a transient interaction between matrix and fractures, especially if one of the three parallel straight lines is missing because of wellbore storage effects or because of the short duration of the test.

The duration of the anomalous slope changes during the transition period is a function of

$$\lambda_{fF} / \lambda_{mF} \quad \text{and} \quad \lambda_{mf} / \lambda_{mf} .$$

Figure 6 presents a comparison of fractures and vugs pressure profiles at different times.

As expected before the homogeneous flow period, vugs pressure drop profiles around the wellbore are lower than fracture profiles. The matrix profiles, not shown in this figure, before the homogeneous period is very small. During the homogeneous flow period, fracture, vugs, and matrix pressure profiles agree. Although profiles computed with the complete analytical solution, given by eq. A-25 are not presented in this figure, they are very close to the numerical inversion profiles.

Using the analytical solution, given by eq. (A-16), short, intermediate, and long time approximations are obtained.

Fig. 7 presents results in term of both the pressure and derivate function.

The number of variables to be defined, three interporosity flow parameters, three interporosity flow parameters, two storativity ratios, wellbore storage constant, and skin factor, makes the use of a type curve matching procedure necessary.

Figures 8 and 9 show two type curves for un connected vugs, with $\lambda_{mf} = 10^{-7}, \omega_F = 10^{-5}$, and considering no wellbore storage and skin effects.

Fig. 8, pressure and pressure derivative curves for different values of λ_{mF} and ω_f, keeping fixed λ_{fF} in 10^{-7}, are presented.

This solution, that also includes a skin in both vugs and fractures, extends the single permeability solution.

The inclusion of vugs skin factor is important because well-connected, large vugs are usually invaded by drilling mud only in a vecinity of the well, never reach the pseudosteady transfer between vugs and fractures.

Figure 10 shows a comparison of production decline results for transient condition with no skin fracture and also for two different skin values, s_{mF} =0.6 and 10; the later results closely correspond to the pseudosteady state flow condition.

Even the type curve matching procedure may be difficult and not unique, it represents an attractive possibility to obtain the distribution of porosity between fractures, vugs, and matrix, and their interaction. This is important because core data underestimate the permeability of vugs zones, and vugs are not always recognized by conventional logs.

Conclusions

The main purpose of this work has been to present a more general transient test analysis for NFR based on the transient interporosity flow, including the matrix and microfracture skin effect.

From the results of this study, the following conclusions can be established:

- The model permits an easy change of the matrix block geometry or vugs.
- Approximate analytical solutions for short and long times are presented; others previously presented solutions are particular cases.
- For decline curve analysis, the use of the Warren and Root Model for the decline analysis of multiple porosity systems can be justified by using a matrix- fracture flow restriction.
- The matrix-fracture and vug-fracture skins can be confirmed by other sources, such as that from thin section of cores.
- The bulk fracture parameters of permeability and the storativity and the outer radius can be estimated through the methodology of this study.
- The estimated flow rate considering transient matrix to fractures transfer and transient microfracture to fracture transient obtained in this work is higher than the value of pseudosteady state given by Rodriguez de la Garza et al.[25]
- It is shown that by using flow tests a better characterization of the naturally fractured reservoir can be achieved.
- **The flow rate give the adequate interporosity (fracture) skin, exposed area transfer and spacing between fractures for modeling the imbibition, for forecasting and develop fields.**

References

1. Camacho V. R., Vasquez C. M. , Castrejón A. R. and Arana O. V.: "Pressure-Transient an Declined-Curve Behavior in Naturally Fractured Vuggy carbonate Reservoirs", SPE Reservoir Evaluation & Eng. (April 2005) 95-111.
2. Rodríguez F.,Arana-Ortiz V. and Cinco Ley H., 2005: "Well Test Characterization of Small-and Large-Scale Secondary Porosity in Naturally fractured Reservoirs", paper SPE 90287 presented at the Annual Technical Conference and Exhibition, Houston, Texas., September 26-29.
3. Cinco Ley, H. and Samaniego, V. F., 1982: "Pressure Transient Analysis for Naturally Fractured Reservoirs", paper SPE 11026. presented at the 57th Annual Fall Technical Conference and Exhibition New Orleans, La., September 26-29.
4. Cinco Ley H., Samaniego, V. F and Kucuk, F., 1985: "The Pressure Transient Behavior for a Naturally Fractured Reservoirs with Multiple Block Size", paper SPE 14168 presented at the Annual Technical Conference and Exhibition, Bakersfield, CA., March 27-29.
5. Gringarten, A., C., 1979: "Flow Tests Evaluation of Fractured Formations", paper presented at the symposium on Recent Trends in Hydrogeology. Berkeley, CA, Feb. 8-9.
6. Herrera, G. R.: "Análisis Petrofísicos de Formaciones Naturalmente Fracturadas", Ph. D. Dissertation, School of Engineering, National University of Mexico (2000).
7. Herrera G. R., Samaniego V. F. and Hernández, F.: "On the Petrophysics of Carbonate Reservoirs Through Whole Core Analysis", paper SPE 28675 presented at the 1994 SPE.
8. Stehfest, H., 1970: "Algorithm 368: "Numerical Inversion of Laplace Transforms", *Communications of the ACM* (Jan.) **13**, 47-49.
9. Warren, J. E. and Root, P. J., 1963: "The Behavior of Naturally Fractured Reservoirs", *SPE Journal (*Sep.), **Vol. 3**, 245-255; *Trans*. AIME, **228**.

Nomenclature

A = drainage area, ft^2.

B = formation volume factor, RB/STB.

c_t = compressibility, psi^{-1}.

C_A = dimensionless pseudo steady state shape factor.

C_{fb} = fracture area; is the ratio between matrix surface and rock volume, ft^{-1}.

h = formation thickness, ft.

H = matrix block size, ft.

In = modified Bessel function, first kind, nth order.

k = permeability, md.

Kn = modified Bessel function, second kind, nth order.

p = pressure, psi.

$\bar{p}$ = Laplace transform of p .

p_{wf} = wellbore flowing pressure, psi.

$q(t)$ = volumetric rate, bbl/day.

N_p = cumulative production, bbl.

n = number of normal set of fractures.

r_D = dimensionless radius.

r_e = outer boundary radius, ft.

r_{eD}' = effective dimensionless well outer radius.

r_w = wellbore radius, ft.

r_w' = effective wellbore radius, ft.

s = Laplace space parameter.

S_f = fracture skin.

S_w = Van Everdingen and Hurst skin factor.

t = time, hours.

t_{DA} = dimensionless time based on drainage area A.

V = ratio of total volume of medium to bulk volume.

x = thickness, ft.

α = interporosity flow shape factor, ft^{-2}.

ς = characteristic dimension of the heterogeneous medium, ft.

λ = dimensionless matrix-fracture permeability ratio, reflects the intensity of the fluid transfer matrix fractures.

η = diffusivity.

μ = viscosity, cp.

ϕ = porosity, fraction.

ω = dimensionless fracture storativity, is the ratio of the storage capacity of the fracture to the total capacity of the medium.

Subscripts

b = bulk (matrix and fractures).

D = dimensionless.

d = damaged zone.

e = external.

f = microfracture

F = fracture

m = matrix

surf = matrix-fracture surface

t = total

Appendix A

General and Approximate Solutions for the Transient Flow of a Fluid in a Naturally Fractured Reservoir, with Transient Interporosity.

Applying the transform to matrix-fracture function:

$$\overline{F}_{mF}(\eta_{mFD},s)=L\left[4\eta_{mFD}\sum_{n=1}^{\infty}e^{-\eta_{mFD}(2n+1)^2\pi^2 t_D}\right]$$
$$=4\eta_{fFD}\sum_{n=1}^{\infty}\frac{1}{s+\eta_{mFD}(2n+1)^2\pi^2} \quad \text{(A-1)}$$

The is Summatory in Eq. (A-1) can be represented by a continuous function:

$$\sum_{n=1}^{\infty}\frac{1}{s+\eta_{mFD}(2n+1)^2\pi^2}=\frac{1}{4\sqrt{s/\eta_{mFD}}}tgh\left(\frac{\sqrt{s/\eta_{mFD}}}{2}\right) \quad \text{(A-2)}$$

Applying the transform microfracture-fracture:

$$\overline{F}_{mF}\left(\eta_{fFD},s\right)=L\left[4\eta_{fFD}\sum_{n=0}^{\infty}e^{-\eta_{fFD}(n)^2\pi^2 t_D}\right]$$
$$=4\eta_{fFD}\sum_{n=0}^{\infty}\frac{1}{s+\eta_{fFD}(n)^2\pi^2} \quad \text{(A-3)}$$

Summatory can be represented by continuous function:

$$\eta_{fFD}\sum_{n=0}^{\infty}\frac{1}{s+\eta_{fFD}(n)^2\pi^2}=\frac{1}{4\sqrt{s/\eta_{mFD}}}\left[ctgh\left(\frac{\sqrt{s/\eta_{mFD}}}{2}\right)-\frac{2}{\sqrt{s/\eta_{mFD}}}\right] \quad \text{(A-4)}$$

Applying the Laplace transform to Eq. (1) that describes the radial flow in the large scale secondary porosity media:

$$\frac{d^2\overline{p_{FD}}(r_D,s)}{dr_D^2}+\frac{1}{r_D}\frac{d\overline{p_{FD}}(r_D,s)}{dr_D}$$
$$-\omega_f(s)C_{fFbD}(s)\left[s\overline{p_{FD}}(r_D,s)-p_{FD}(r_D,0)\right]\frac{\overline{F}_{fF}(\eta_{fFD},s)}{1+S_{fF}\overline{F}_{fF}(\eta_{fFD},s)}$$
$$-\left[1-\omega(s)-\omega_F(s)\right]C_{mFbD}(s)\left[s\overline{p_{FD}}(r_D,s)-p_{FD}(r_D,0)\right]\frac{\overline{F}_{mF}(\eta_{mFD},s)}{1+S_{mF}\overline{F}(\eta_{mFD},s)}$$
$$=\omega_F(s)\left[s\overline{p_{FD}}(r_D,s)-p_{FD}(r_D,0)\right] \quad \text{(A-5)}$$

Replacing the initial condition given by Eq. (9) in the right hand side of Eq. (A-5):

$$\frac{d^2\overline{p}_{FD}(r_D,s)}{dr_D^2}+\frac{1}{r_D}\frac{d\overline{p}_{FD}(r_D,s)}{dr_D}$$
$$-\omega_f(s)C_{fFbD}(s)s\overline{p}_{FD}(r_D,s)\frac{\overline{F}_{fF}(\eta_{fFD},s)}{[1+S_{fF}\overline{F}_{fF}(\eta_{fFD},s)]}$$
$$-\left[1-\omega_f(s)-\omega_F(s)\right]C_{mFbD}(s)s\overline{p}_{FD}(r_D,s)\frac{\overline{F}_{mF}(\eta_{mFD},s)}{[1+S_{mF}\overline{F}_{mF}(\eta_{mFD},s)]}$$
$$=\omega_F(s)s\overline{p}_{FD}(r_D,s) \quad \text{(A-6)}$$

Eq. (A-6) can be written as follows:

$$\frac{d^2\overline{p_{FD}}(r_D,s)}{dr_D^2}+\frac{1}{r_D}\frac{d\overline{p_{FD}}(r_D,s)}{dr_D}-sf(s)\overline{p_{FD}}(r_D,s)=0, \quad \text{(A-7)}$$

where:

$$f(s)=\omega_F(s)+\omega_f(s)C_{fFbD}(s)\frac{\overline{F}_{fF}(\eta_{fFD},s)}{1+S_{fF}\overline{F}_{fF}(\eta_{fFD,S})}$$
$$+[1-\omega_f(s)-\omega_F(s)]C_{mFbD}(s)\frac{\overline{F}_{mF}(\eta_{mFD,S})}{1+S_{mF}\overline{F}_{mF}(\eta_{mFD,S})}. \quad \text{(A-8)}$$

The general solution of the equation of flow in the large scale secondary porosity medium is:

$$\overline{p}_{FD}(r_D,s)=AIo\left(r_D\sqrt{sf(s)}\right)+BKo\left(r_D\sqrt{sf(s)}\right). \quad \text{(A-9)}$$

Applying the Laplace transform to the boundary conditions given by Eqs. (10) and (11):

$$\frac{d\overline{p}_{FD}(1,s)}{dr_D}=-\frac{1}{s} \quad ; \quad \text{(A-10)}$$

$$\lim_{r_D\to\infty}\overline{p}_{FD}(r_D,s)=0. \quad \text{(A-11)}$$

Eqs. (A-9) to (A-11) gives the Laplace space dimensionless pressure in the large scale secondary porosity:

$$\bar{p}_{FD}(r_D, s) = \frac{1}{s\sqrt{sf(s)}} \frac{Ko\left(r_D\sqrt{sf(s)}\right)}{K_1\left(\sqrt{sf(s)}\right)},$$

(A-12)

where:

$$f(s) = \omega_F(s) + \omega_f(s) C_{fFbD}(s) g_1(s)$$

$$+ [1 - \omega_f(s) - \omega_F(s)] C_{mFbD}(s) g_2(s)$$

(A-13)

Where the parameters C_{mFbD} and C_{fFbD} are given by Eqs. (32) and (34), and the transient transfer functions including the skin are:

$$g_1(s) = \frac{\eta_{fFD}^{3/2} \tanh(0.5\sqrt{s/\eta_{fFD}})}{\sqrt{s} + S_{fF}\eta_{mD}^{3/2} \tanh(0.5\sqrt{s/\eta_{fFD}})} \quad \text{(A-14)}$$

$$g_2(s) = \frac{\eta_{mFD}^{3/2} \tanh(0.5\sqrt{s/\eta_{mFD}})}{\sqrt{s} + S_{mF}\eta_{mFD}^{3/2} \tanh(0.5\sqrt{s/\eta_{mFD}})}$$

(A-15)

The dimensionless wellbore pressure can be expressed considering $r_D = 1$ in Eq. (A-10):

$$\bar{p}_{FwD}(s) = \frac{1}{s\sqrt{sf(s)}} \frac{Ko\left(\sqrt{sf(s)}\right)}{K_1\left(\sqrt{sf(s)}\right)},$$

(A-16)

where:

$$f(s) = \omega_F(s) + \omega_f(s) C_{fFbD}(s) \frac{\eta_{fFD}^{3/2}}{\sqrt{s} + S_{fF}\eta_{mD}^{3/2}}$$

$$+ [1 - \omega_f(s) - \omega_F(s)] C_{mFbD}(s) \frac{\eta_{mFD}^{3/2}}{\sqrt{s} + S_{mF}\eta_{mFD}^{3/2}}.$$

(A-17)

Complete Analytical Solution

The following Bessel function relations are valid for big arguments:

$$K_1\left(\sqrt{s[A]}\right) \approx \frac{1}{\sqrt{s[A]}}$$

(A-18)

$$K_0\left(\sqrt{s[A]}\right) \approx -\ln\left(\frac{e^\gamma}{2}\sqrt{s[A]}\right).$$

(A-19)

Substituting the approximations given by Eqs. (A-18) and
(A-19) in Eq. (A-16):

$$\bar{p}_{FwD}(s) = \frac{-\ln\left(\frac{e^\gamma}{2}\sqrt{sf(s)}\right)}{s}.$$

(A-20)

This Eq. A-20 can be expressed:

$$\bar{p}_{FwD}(s) = \frac{-\frac{1}{2}\ln\left(\frac{e^{2\gamma}s}{4} f(s)\right)}{s} = -\frac{1}{2}\frac{\ln\left(\frac{e^{2\gamma}s}{4}\right)}{s} - \frac{1}{2}\frac{\ln(f(s))}{s}$$

(A-21)

$$\bar{p}_{FwD}(s) = -\frac{1}{2}\frac{\ln\left(e^{2\gamma}s/4\right)}{s}$$

$$-\frac{1}{2}\frac{\ln\left(\omega_F + \omega_f C_{fFbD}\frac{\eta_{fFD}^{3/2}}{\sqrt{s}+S_{fF}\eta_{mD}^{3/2}} + [1-\omega_f-\omega_F]C_{mFbD}\frac{\eta_{mFD}^{3/2}}{\sqrt{s}+S_{mF}\eta_{mFD}^{3/2}}\right)}{s}$$

(A-22)

Using different functions of s:

$$\bar{p}_{FwD}(s) = -\frac{1}{2}\frac{\ln\left(\frac{e^{2\gamma}s}{4}\right)}{s} - \frac{1}{2}\frac{\ln\left(\frac{A\omega_F + B + C}{A}\right)}{s}$$

where:

$$A = s + \left[S_{fF}\eta_{mD}^{3/2} + S_{mF}\eta_{mFD}^{3/2}\right]\sqrt{s} + S_{fF}S_{mF}\eta_{mD}^{3/2}\eta_{mFD}^{3/2}$$

$$B = \omega_f C_{fFbD}\eta_{fFD}^{3/2}\left[\sqrt{s} + S_{mF}\eta_{mFD}^{3/2}\right]$$

$$C = [1 - \omega_f - \omega_F] C_{mFbD}\eta_{mFD}^{3/2}\left[\sqrt{s} + S_{fF}\eta_{mD}^{3/2}\right]$$

(A-23)

Rewritten the solution:

$$\bar{p}_{FwD}(s) = -\frac{1}{2}\frac{\ln\left(e^{2\gamma}s/4\right)}{s} - \frac{1}{2}\frac{\ln\left(A\omega_F + B + C\right)}{s} + \frac{1}{2}\frac{\ln(A)}{s}$$

(A-24)

The complete solution in real time is:

$$p_{FwD}(t_D) = \frac{1}{2}\left[\ln(t_D) + 0.80907 + Ei\left(\frac{-C_{fFbDi}\eta_{fFbD}t_D}{S_{fF}\left[1-\omega_{fi}-\omega_{Fi}\right]}\right)\right]$$

$$+\frac{1}{2}\left[-Ei\left(\frac{-S_{fF}t_D}{C_{fFbD}\eta_{fFbD}\omega_f\left[1-\omega_f-\omega_F\right]}\right)+Ei\left(\frac{-S_{mF}t_D}{C_{mFbD}\eta_{mFbD}\left[1-\omega_f-\omega_F\right]}\right)\right]$$

$$+\frac{1}{2}\left[-Ei\left(\frac{-S_{mF}t_D}{C_{mFbD}\eta_{mFbD}\left[1-\omega_f-\omega_F\right]^2}\right)\right]$$

(A-25)

Approximate Analytical solution for short times

For small arguments, the function $f(s)$ given by Eq. (A-17) can be expressed:

$$\lim_{s\to\infty} f(s) = \lim_{s\to\infty}\ \omega_F + \lim_{s\to\infty}\frac{[1-\omega]C_{FbD}}{4}\frac{\sqrt{\eta_{mD}}}{\sqrt{s}}\left[\tanh\left(\sqrt{s/\eta_{mD}}/2\right)\right]$$

$$+\lim_{s\to\infty}\frac{[1-\omega]C_{mFbD}}{4}\frac{\sqrt{\eta_{mFbD}}}{\sqrt{s}}\left[\tanh\left(\sqrt{s/\eta_{mFbD}}/2\right)\right] = \omega_F .$$

(A-26)

Replacing this limit for the transfer function in the wellbore pressure given by Eq. (A-16):

$$\bar{p}_{FwD}(s) = \frac{1}{s\sqrt{s\omega_F}}\frac{K_0\left(\sqrt{s\omega_F}\right)}{K_1\left(\sqrt{s\omega_F}\right)}.$$

(A-27)

The following approximations for the Bessel functions are valid for small arguments:

$$K_0\left(\sqrt{s\kappa}\right) \approx -\ln\left(e^{\gamma}\sqrt{s\omega_F}/2\right),$$

(A-28)

$$K_1\left(\sqrt{s\kappa}\right) \approx \frac{1}{\sqrt{s\omega_{Fi}}}.$$

(A-29)

Replacing the approximations given by Eqs. (A-28) and (A-29) in Eq. (A-16):

$$\bar{p}_{FwD}(s) = \frac{-\ln\left(\frac{e^{\gamma}}{2}\sqrt{s\omega_{Fi}}\right)}{s}.$$

(A-30)

The inversion of Eq. (A-30) results in the solution for early times:

$$p_{FwD}(t_D) = \frac{1}{2}\left[\ln\left(\frac{t_D}{\omega_{Fi}}\right) + 0.80907\right]$$

(A-31)

Approximate Analytical solution for long times:

$$\lim_{s\to 0} f(s) = \lim_{s\to 0}\ \omega + \lim_{s\to 0}\frac{[1-\omega]C_{FbD}}{4}\frac{\sqrt{\eta_{mD}}}{\sqrt{s}}\left[\tanh\left(\frac{\sqrt{s/\eta_{mD}}}{2}\right)\right]$$

(A-32)

For small arguments $\sqrt{s/\eta_{mD}}/2$:

$$\lim_{s\to 0} f(s) = \omega + \frac{[1-\omega]C_{FbD}}{8}\frac{\sqrt{\eta_{mD}}}{\sqrt{s}}\frac{\sqrt{s}}{\sqrt{\eta_{mD}}} \approx 1$$

(A-33)

Replacing the is limit given by Eq. (A-32) in the wellbore pressure:

$$\bar{p}_{FwD}(s) = \frac{1}{s\sqrt{s}}\frac{K_0\left(\sqrt{s}\right)}{K_1\left(\sqrt{s}\right)}.$$

(A-34)

The following approximations for the Bessel functions are valid for small arguments (Eqs. A-28 and A-29):

$$K_0\left(\sqrt{s}\right) \approx -\ln\left(e^{\gamma}\sqrt{s}/2\right)$$

(A-35)

$$K_1\left(\sqrt{s\kappa}\right) \approx \frac{1}{\sqrt{s\kappa}}$$

(A-36)

Substituting Eqs. (A-35) and (A-36) in Eq. (A-16):

$$\bar{p}_{FwD}(s) = \frac{-\ln\left(e^{\gamma}\sqrt{s\kappa}/2\right)}{s}.$$

(A-37)

The inversion of this expression results in Eq. (A-38):

$$p_{FwD}(t_D) = \frac{1}{2}\left[\ln(t_D) + 0.809071\right].$$

(A-38)

a) Core with both horizontal fractures and vertical fractures while connected to vugs of several sizes.
b) Net of fractures in vertical planes connecting vugs.
c) System of conjugate fractures connected to vugs.

Fig. 1 Photographs for whole cores of reservoir A with strong changes with the time.

a) Sealing fractures with calcite and early dolomitization.
b) Fracture System and vugs
c) Vugs plane in the same direction of fractures plane.

Fig. 2 Photographs for whole cores of reservoir B.

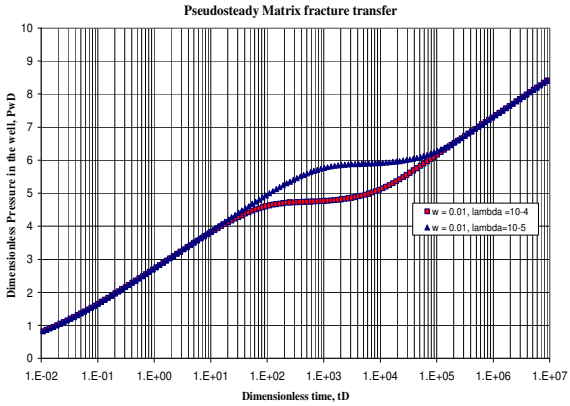

Fig. 3. Pseudosteady matrix-fracture flow for constant omega and two lambda in a semilog graph.

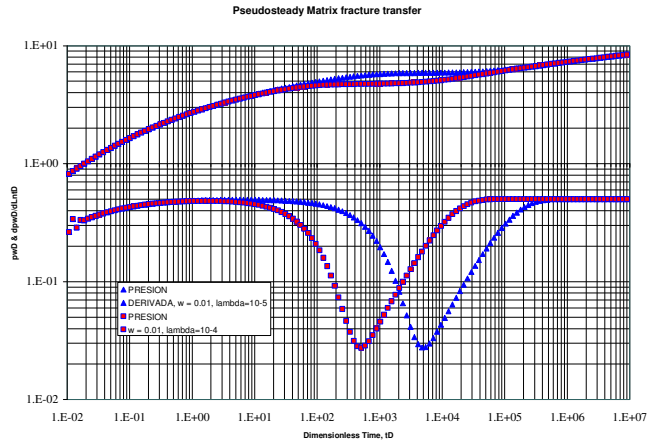

Fig. 4. Pseudosteady matrix-fracture flow for the same omega and two lambda in a log-log graph.

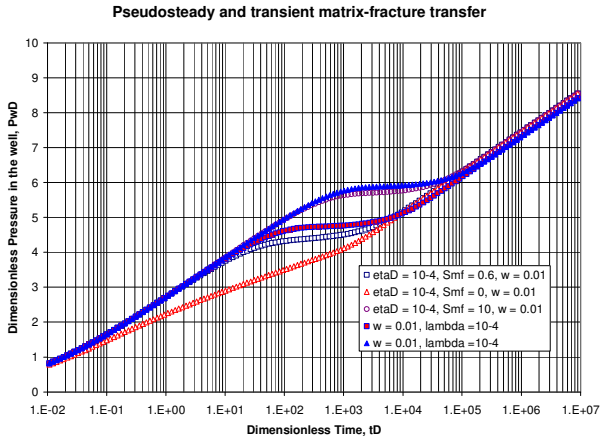

Fig. 5. Pseudosteady and Transient matrix-fracture with interporosity skin in a semilog graph. It is necessary to use a other sources for to confirm omega and lambda.

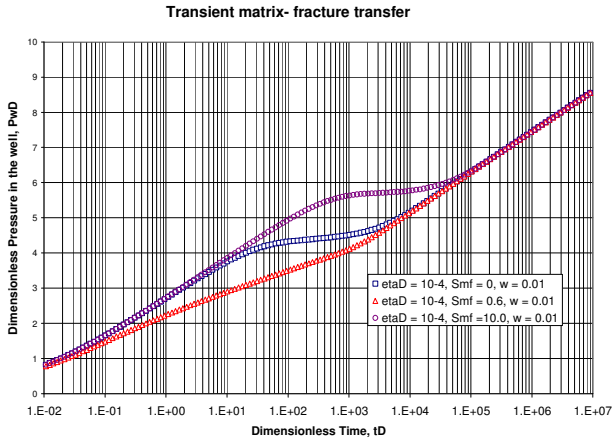

Fig. 5. Transient matrix-fracture with interporsity skin. The transition period exhibit a straight line with slope equal to one half the slope of the classic parallel semilog straight lines, in a semilog graph.

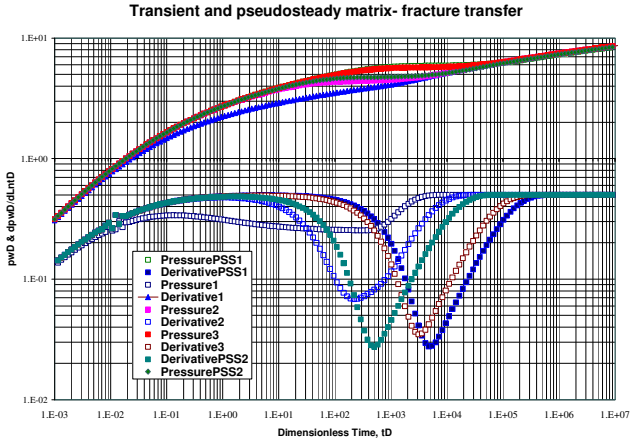

Fig. 8. Pseudosteady and Transient matrix-fracture with interporosity skin in a log-log graph. It is necessary to use a other sources for to confirm omega and lambda.

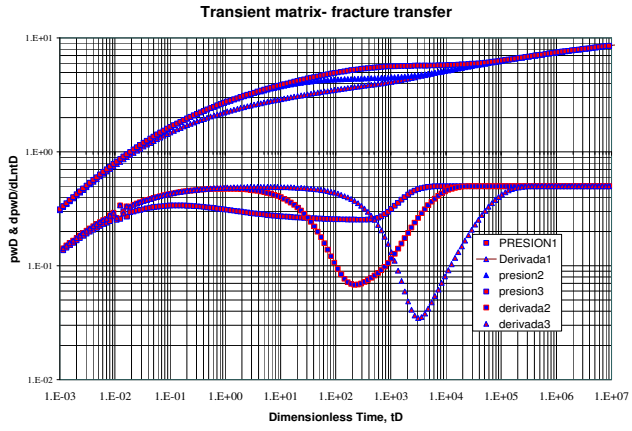

Fig. 6. Transient matrix-fracture with interporsity skin. The transition period exhibit a “u” form without skin and “v” for skin =10 in a log-log graph.

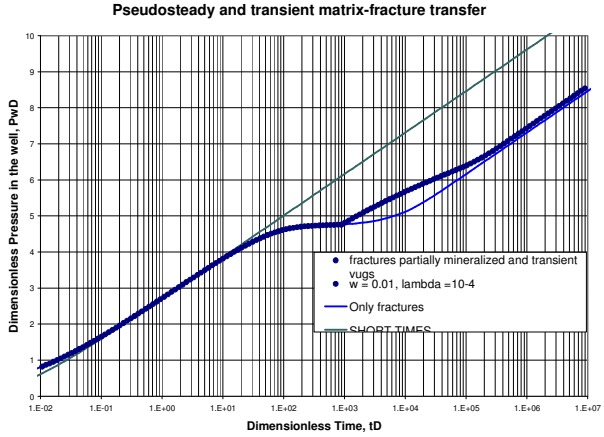

Fig. 9 Two behavior simultaneously in the transition period: Pseudosteady and Transient matrix-fracture in

a log-log graph. Transient matrix fracture with skin in a fractures and transient in vugs.

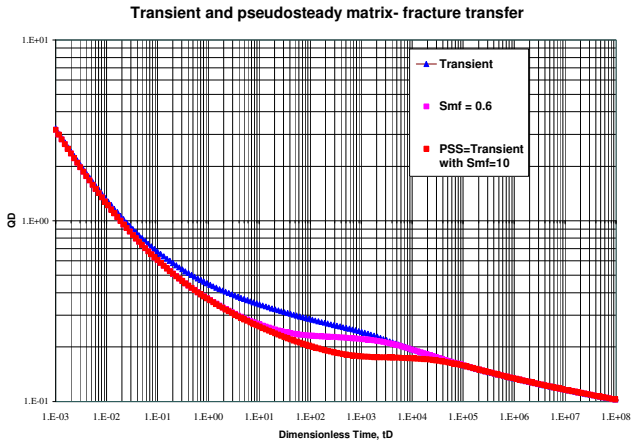

Fig. 10. Pseudsteady matrix fracture transfer give the minimum response in production, the transient matrix fracture transfer give the maximum response in production, the real production must be the correct skin between matrix and fractures.